International Journal of Pharmaceutics 432 (2012) 99–104

Contents lists available at SciVerse ScienceDirect

International Journal of Pharmaceutics

journal homepage: www.elsevier.com/locate/ijpharm

Pharmaceutical Nanotechnology

Multifunctionalized mesoporous silica nanoparticles for the *in vitro* treatment of retinoblastoma: Drug delivery, one and two-photon photodynamic therapy

Magali Gary-Bobo[a], Youssef Mir[b], Cédric Rouxel[b], David Brevet[c], Ouahiba Hocine[c], Marie Maynadier[a], Audrey Gallud[a], Afitz Da Silva[a], Olivier Mongin[b], Mireille Blanchard-Desce[b,*], Sébastien Richeter[c], Bernard Loock[d,e], Philippe Maillard[d,e], Alain Morère[a], Marcel Garcia[a,*], Laurence Raehm[c], Jean-Olivier Durand[c,*]

[a] *Institut des Biomolécules Max Mousseron UMR 5247 CNRS, Université Montpellier 1, Université Montpellier 2, Faculté de Pharmacie, 15 Avenue Charles Flahault, 34093 Montpellier Cedex 05, France*
[b] *Chimie et Photonique Moléculaires, CNRS UMR 6510, Campus de Beaulieu, Université Rennes 1, 35042 Rennes Cedex, France*
[c] *Institut Charles Gerhardt Montpellier, UMR 5253 CNRS-UM2-ENSCM-UM1, CC1701 Place Eugène Bataillon, 34095 Montpellier Cedex 05, France*
[d] *UMR 176 CNRS/Institut Curie, Institut Curie, Bât 110-112, Université Paris-Sud, F-91405 Orsay, France*
[e] *Institut Curie, Section de Recherches, Centre Universitaire, Université Paris-Sud, F-91405 Orsay, France*

ARTICLE INFO

Article history:
Received 22 February 2012
Received in revised form 17 April 2012
Accepted 21 April 2012
Available online 28 April 2012

Keywords:
Mesoporous silica nanoparticles
Two-photon
Photodynamic therapy
Drug delivery
Mannose
Galactose
Targeting
Retinoblastoma

ABSTRACT

In this work, we focused on mesoporous silica nanoparticles (MSN) for one photon excitated photodynamic therapy (OPE-PDT) combined with drug delivery and carbohydrate targeting applied on retinoblastoma, a rare disease of childhood. We demonstrate that bitherapy (camptothecin delivery and photodynamic therapy) performed with MSN on retinoblastoma cancer cells was efficient in inducing cancer cell death. Alternatively MSN designed for two-photon excited photodynamic therapy (TPE-PDT) were also studied and irradiation at low fluence efficiently killed retinoblastoma cancer cells.

1. Introduction

Retinoblastoma (RB), a rare disease, is the most common primary intraocular tumor of childhood (Doz, 2006; Houston et al., 2011) with an incidence of 1 for 15,000–20,000 births. The disease is associated with a mutation of the RB gene, RB1 in about 40% of the patients with bilateral RB (Aerts et al., 2006; Friend et al., 1986). The mutation is also present in 15% of the patients with unilateral RB. The vital prognosis related to RB itself is excellent, with cure rates greater than 95% in industrialized countries. However, due to the risk of secondary malignant neoplasms occurring years after treatment, long-term survival in patients with the RB1 gene mutation is reduced, which represent the leading cause of death in patients with hereditary RB (Aerts et al., 2004; Wong et al., 1997). The current therapeutic treatments available to cure patients with RB include enucleation or conservative treatment using, cryotherapy (Shields et al., 1993) local thermotherapy (Lumbroso et al., 2002; Murphree et al., 1996) or brachytherapy (Shields et al., 2001b). To reduce tumor size, primary chemotherapy is often necessary and further makes the tumor accessible to conservative treatment (Chantada et al., 2005; Levy et al., 1998; Murphree et al., 1996; Rodriguez-Galindo et al., 2003; Shields et al., 2001a). The potential risks of late effects associated with chemotherapy and carboplatin include increased risk of second cancer in patients with RB1 gene mutation, as well as short-term important side effects. External-beam radiotherapy is increasingly restricted due to the risk of late effects, such as secondary sarcoma (Kleinerman et al., 2005). In this context, more efficient treatments allowing to decrease the dosage of the anticancer drug and to deliver it at the tumor site to avoid side-effects are of importance. Furthermore, an approach which would combine drug delivery with another therapy such as photodynamic therapy (PDT) (which is non mutagenic), would

* Corresponding authors. Tel.: +33 (0)4 67 14 45 01; fax: +33 (0)4 67 14 38 52.
E-mail addresses: mireille.blanchard-desce@u-bordeaux1.fr (M. Blanchard-Desce), Marcel.garcia@inserm.fr (M. Garcia), durand@univ-montp2.fr (J.-O. Durand).

0378-5173/$ – see front matter © 2012 Elsevier B.V. All rights reserved.
http://dx.doi.org/10.1016/j.ijpharm.2012.04.056

further improve the treatment of RB. For this purpose, tremendous efforts have been devoted to nanoparticles. In this field, mesoporous silica nanoparticles (MSN) are highly promising due to their interesting properties (Rosenholm et al., 2010; Slowing et al., 2010) (monodispersity, high specific surface area, tunable pore size and diameter, versatile functionalization). We have demonstrated the potential of MSN for bi-therapy *in vitro* by combining OPE-PDT (one photon excitation-PDT), drug delivery, and targeting with galactose (Gary-Bobo et al., 2012). We showed that those MSN led to a dramatic enhancement of cancer cell death compared to separate treatments. To further enhance the precision of PDT, particularly for small tumors where focal therapy is needed, two-photon excitation (TPE) combined with PDT is of current interest (Collins et al., 2008; Khurana et al., 2009; Starkey et al., 2008). Indeed TPE-PDT offers new perspectives due to the unique properties it provides such as 3D spatial resolution and increased penetration depth. We (Gary-Bobo et al., 2011) and others (Cheng et al., 2011) have very recently designed MSN for TPE-PDT *in vitro* and *in vivo*. Combined with targeting with mannose, the MSN were very efficient for TPE-PDT on breast and colon cancer cells (Gary-Bobo et al., 2011). Furthermore, mannose or galactose-functionalized porphyrins have been demonstrated to be efficient for OPE-PDT *in vitro* (Lavielle et al., 2006) and *in vivo* (Lupu et al., 2009), probably due to an active endocytosis involving lectins at the surface of Y-79 RB tumor cells. Therefore, in connection with these works, we present here our results with MSN combining OPE-PDT, camptothecin (CPT) delivery and targeting with mannose or galactose on retinoblastoma cells Y-79. We also studied TPE-PDT on these cells with MSN encapsulating a photosensitizer engineered for TPE and functionalized with mannose on the surface.

2. Material and methods

2.1. Synthesis of MSN

MSN-FITC (Hocine et al., 2010), **MSN-FITC-man** (Hocine et al., 2010), **MSN-FITC-gal** (Gary-Bobo et al., 2012), **MSN-PS-gal** (Gary-Bobo et al., 2012), **MSN-PS-gal-CPT** (Gary-Bobo et al., 2012), **MSN-2hν** (Gary-Bobo et al., 2011), **MSN-2hν-man** (Gary-Bobo et al., 2011), were already prepared and used in our previous work.

Synthesis of MSN-PS-man. The synthesis was already described in reference Brevet et al. (2009). Briefly.

2.1.1. Preparation of MSN-PS

5.4 mg (5.87 μmol) of anionic porphyrin were dissolved in 1 mL of ethanol. 7.25 μL (5 eq.) of isocyanatopropyltriethoxysilane and 4.1 μL (4 eq.) of diisopropylethylamine were added. The reaction was stirred at room temperature for 12 h. 646 mg (1.8 mmol) of CTAB were dissolved in 40 mL of 0.2 M NaOH at 25 °C. The silylated porphyrin was added to this mixture and 3.5 mL (15.7 mmol) of tetraethoxysilane (TEOS) were added dropwise. After 40 s, 260 mL of deionised water were added to the mixture. The reaction was stirred for 6 min at 25 °C then rapidly neutralized to pH 7 by addition of 0.2 M HCl. Nanoparticles were obtained after centrifugation (10 min, 20,000 rpm), put in suspension in ethanol under ultrasounds and then centrifuged. Specific surface area (860 $m^2\,g^{-1}$), loading of **PS** (5.12 $\mu mol\,g^{-1}$).

2.1.2. Preparation of *MSN-PS-NH$_2$*

500 mg of **MSN-PS** were put in suspension in 10 mL H_2O under ultrasounds for 1 h. Then we added dropwise 800 μL of aminopropyltriethoxysilane APTS (2.76 eq.). This solution was stirred for 1 min and after the pH was adjusted to 7 by addition of 0.2 M HCl. The reaction was stirred at RT for 20 h. Nanoparticles were centrifuged (10 min, 20,000 rpm) and washed with EtOH and dried under vacuum.

Microanalysis: % C: 10.59; % H: 3.30; % N: 1.84.

Loading of APTS: 1.38 $mmol\,g^{-1}$.

2.1.3. Preparation of *MSN-PS-man*

200 mg of **MSN-PS-NH$_2$** were put in suspension in 10 mL EtOH. 55 mg (0.14 mmol) of p-[N-(2-ethoxy-3,4-dioxycyclobut-1-enyl)amino]phenyl-α-D-mannopyranoside were dissolved in 10 mL of a mixture EtOH/H_2O (3/2, v/v). This solution was added dropwise to the suspension of nanoparticles. 500 μL of triethylamine were added and the suspension was stirred for 15 h at room temperature. After centrifugation (10 min, 20,000 rpm), nanoparticles were washed one time with water and with EtOH. CTAB was extracted with 30 mL of solution of EtOH (96%)/NH_4NO_3 (0.03 $mol\,L^{-1}$) for 1 h under ultrasounds. After centrifugation, the extraction procedure was repeated two times, and then nanoparticles were washed three times in EtOH. They were dried under vacuum.

Surface area (860 $m^2\,g^{-1}$); pore diameter (2.5 nm); pore volume (0.57 $cm^3\,g^{-1}$); loading of mannose (0.276 $mmol\,g^{-1}$).

2.1.4. *MSN-PS-man-CPT*

30 mg of **MSN-PS-man** were suspended and stirred in a solution of camptothecin (3 mg, 8.6 μmol) in 1.8 mL DMSO overnight at room temperature. After centrifugation (10 min, 25,000 rpm) nanoparticles were washed with water, centrifuged (2 cycles) and dried under vacuum.

Titration (UV–vis) gave 11.22 $\mu mol\,g^{-1}$ camptothecin loaded in the MSN.

2.2. Cell culture conditions

Human retinoblastoma (Y-79) cancer cells were purchased from ATCC (American Type Culture Collection, Manassas, VA). Cells were cultured in RPMI culture medium supplemented with 20% fetal bovine serum, 100 U mL^{-1} penicillin and 100 $\mu g\,mL^{-1}$ streptomycin and allowed to grow in humidified atmosphere at 37 °C under 5% CO_2.

2.3. TPE-PDT, OPE-PDT and phototoxicity measurement

For TPE irradiation, Y-79 cells were seeded into 384 multi-well glass bottom (thickness 0.17 mm), with a black polystyrene frame, 2000 cells per well in 50 μL culture medium and allowed to grow for 24 h. Cells were then incubated for 24 h with or without 20 $\mu g\,mL^{-1}$ MSN. After incubation with MSN, cells were submitted or not to laser irradiation. Two-photon irradiation was then performed on a confocal microscope equipped with a mode-locked Ti:sapphire laser generating 100 fs wide pulses at a 80 MHz rate. The laser beam is focused by a microscope objective lens (10×, NA 0.4). The wells were irradiated at 760 nm by 3 scans of 1.25 s each at an average power of 80 mW (measured with a thermoelectric optical energy meter) and the surface of the scanned areas was 1.5 mm × 1.5 mm (mean energy of 10.6 $J\,cm^{-2}$).

For monophotonic irradiation, Y-79 cells were seeded into 96-well plates at 2×10^4 cells per well in 100 μL culture medium and allowed to grow for 24 h. Then cells were incubated for 24 h with or without 20 $\mu g\,mL^{-1}$ MSN. After incubation, cells were submitted or not to laser irradiation for 30 min (650 nm; 50 mW cm^{-2}, 90 J cm^{-2}).

Two day after irradiations (one or two photon), a MTS assay was performed to evaluate the phototoxicity of MSN. Briefly, MTS assay was performed by adding 20 μL of 3-(4,5-dimethylthiazol-2-yl)-5-(3-carboxymethoxyphenyl)-2-(4-sulfophenyl)-2H-tetrazolium salt (CellTiter 96 Aqueous One Solution Reagent from Promega) solution. Cells were incubated 3 h at 37 °C and the absorbance was read at 490 nm in a plate reader to determine the formazan

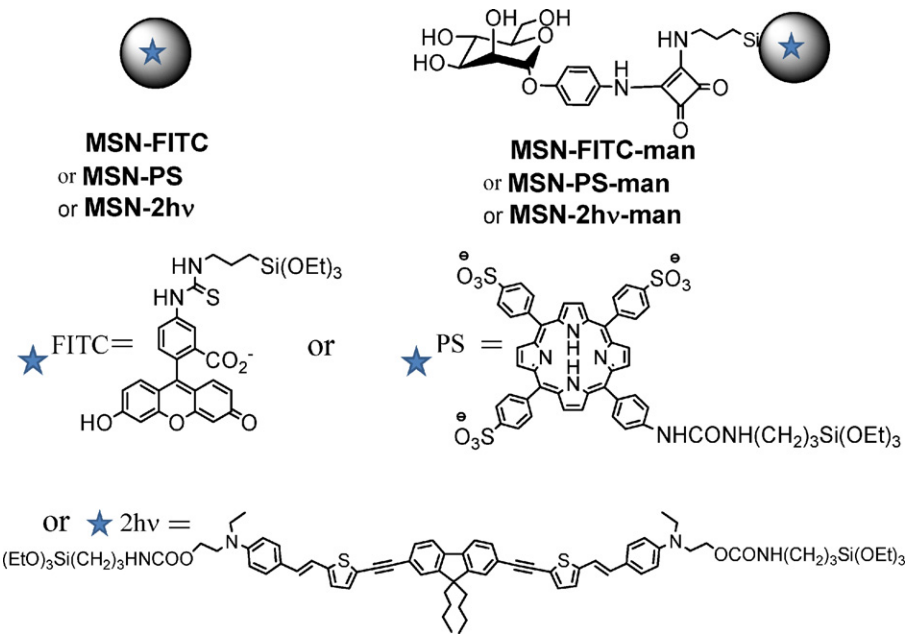

Scheme 1. Structures of **MSN-FITC**, **MSN-PS**, **MSN-2h*ν***, **MSN-FITC-man**, **MSN-PS-man** and **MSN-2h*ν*-man** nanoparticles. The carbohydrate moiety (α-D-mannose, **man**) was covalently anchored on the surface of the MSN.

concentration, which is proportional to the number of living cells.

2.4. Cytotoxicity assay for drug delivery

For these experiments, Y-79 cells were seeded into 96-well plates at 2×10^4 cells per well in 100 μL culture medium and allowed to grow for 24 h. Then cells were incubated at different times with or without 20 μg mL^{-1} MSN. To evaluate the cytotoxicity of MSN, a MTS assay was performed as previously described.

2.5. Confocal analysis of fluorescent MSN

Two days prior to the experiment, Y-79 cells were seeded onto bottom glass dishes (World Precision Instrument, Stevenage, UK) previously coated for 1 h at 37 °C with polylysine 50 μg mL^{-1} for cell adherence, at a density of 10^6 cells cm^{-2}. 24 h after seeding, cells were treated with 20 μg mL^{-1} fluorescent labeled MSN. On the day of the experiment, cells were washed once and incubated in 1 mL red-free medium. Thirty minutes before the end of incubation, cells were loaded with Hoechst 33342 (Invitrogen, Cergy Pontoise, France) for nuclear staining at a final concentration of 5 μg mL^{-1}. For membrane labeling, a Vybrant lipid-raft labeling kit (Invitrogen) was used as described by the manufacturer. Before visualization, cells were washed gently with phenol red-free DMEM. Cells were then scanned with a LSM 5 LIVE confocal laser scanning microscope (Carl Zeiss, Le Pecq, France), with a slice depth (Z stack) of 0.67 μm (Vezenkov et al., 2010).

2.6. Statistical analysis

Statistical analysis was performed using the Student's *t* test to compare paired groups of data. A *p* value of <0.05 was considered to be statistically significant.

3. Results and discussion

The nanoparticles used in this study are depicted in Schemes 1 and 2.

MSN-FITC nanoparticles were used for confocal experiments in order to analyze the endocytosis of the MSN. **MSN-PS** nanoparticles were studied for both one photon PDT and one photon PDT combined to drug delivery. **MSN-2h*ν*** nanoparticles were used for two-photon PDT experiments.

3.1. Internalization and subcellular localization of functionalized MSN by confocal microscopy

The cell distribution of **MSN-FITC**, **MSN-FITC-man** and **MSN-FITC-gal** in Y-79 cells was studied. **MSN-FITC**, **MSN-FITC-man** and **MSN-FITC-gal** were incubated for 16 h with Y-79 cells and then nucleus and membranes were stained as described in experimental section (Fig. 1).

Merged image showed that MSN functionalized with galactose or mannose, were efficiently internalized in comparison with unfunctionalized ones (Fig. 1). The addition in culture medium of an excess of mannose or galactose inhibits near totally this intracellular uptake demonstrating that these MSN were captured by a specific endocytosis involving mannose or galactose receptors. These results are consistent with the work of Griegel et al. (1989) who established that human retinoblastoma cells express sugar receptors that exhibit a preferential affinity for galactose and mannose residues.

3.2. Monosaccharide-functionalized MSN and drug delivery

The pores of **MSN-PS-gal** and **MSN-PS-man** were loaded with camptothecin following the method originally developed by Zink and Tamanoi (Lu et al., 2007) to lead to **MSN-PS-gal-CPT** and **MSN-PS-man-CPT**. To study the cytotoxicity induced by these MSN, Y-79 cell lines were treated with MSN at 20 μg mL^{-1} and cell viability was monitored by using MTS assay. We have first verified that 20 μg mL^{-1} MSN without camptothecin were not cytotoxic for cells

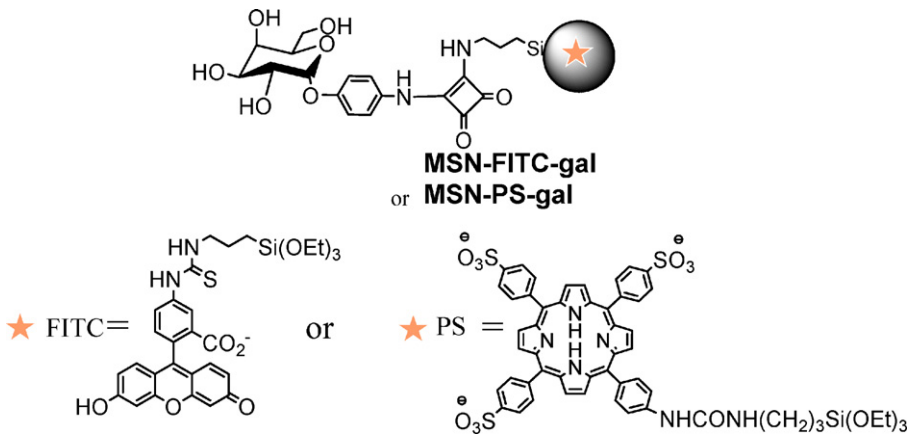

Scheme 2. Structures of **MSN-FITC-gal** and **MSN-PS-gal** nanoparticles. The carbohydrate moiety (α-D-galactose, **gal**) was covalently anchored on the surface of the MSN.

(data not shown). Results showed that **MSN-man-CPT** and **MSN-gal-CPT** induced 35% and 34% of cell death respectively, after 3 days of incubation (Table 1). These results confirmed the previous studies (Gary-Bobo et al., 2012; Liong et al., 2008; Lu et al., 2007) who showed the potential of MSN for drug delivery with poorly water-soluble drugs, and demonstrated the efficiency of camptothecin delivery in Y-79 cells line by MSN functionalized with carbohydrates.

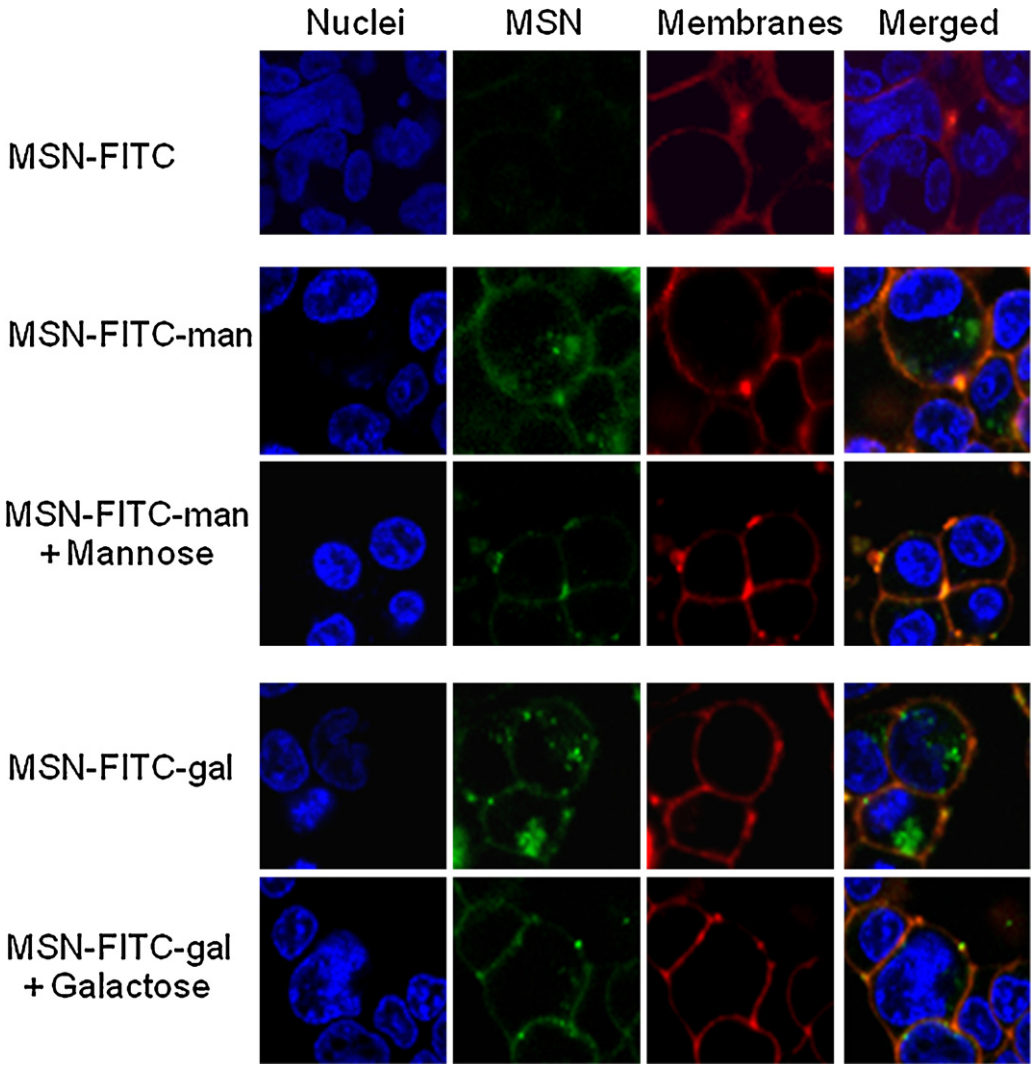

Fig. 1. Confocal microscopy images of living Y-79 retinoblastoma cells, incubated for 16 h with **MSN-FITC** or **MSN-FITC-man** or **MSN-FITC-gal**, in presence or absence of 10 mM mannose or galactose. Merged pictures demonstrated the localization of MSN inside the cells at 37 °C. Images are representative of at least 3 independent experiments.

Table 1
Cytotoxic effect of MSN-camptothecin on human retinoblastoma cells. Y-79 cells were incubated with **MSN** for 1, 2 or 3 days. The level of cell death (%) was measured by the MTS assay.

Living Y-79 cells (%)	Days			
	0	1	2	3
MSN-man-CPT	100 ± 4	87 ± 4	74 ± 3*	65 ± 5*
MSN-gal-CPT	100 ± 4	90 ± 2	76 ± 3*	66 ± 2*

Data are mean ± SD of 3 independent experiments.
* $p < 0.05$ statistically different from control.

3.3. Combining PDT and drug delivery in the same MSN

We next examined targeted MSN combining drug delivery and OPE-PDT (Fig. 2). Cells were treated with photo-activable nanoparticles functionalized with mannose or galactose and containing or not camptothecin. For this experiment, Y-79 cells were incubated for 24 h with 20 μg mL^{-1} MSN and irradiated for 30 min (650 nm; 50 mW cm^{-2}). A MTS assay was performed 2 days after irradiation to assess the induced cytotoxicity. We have verified that

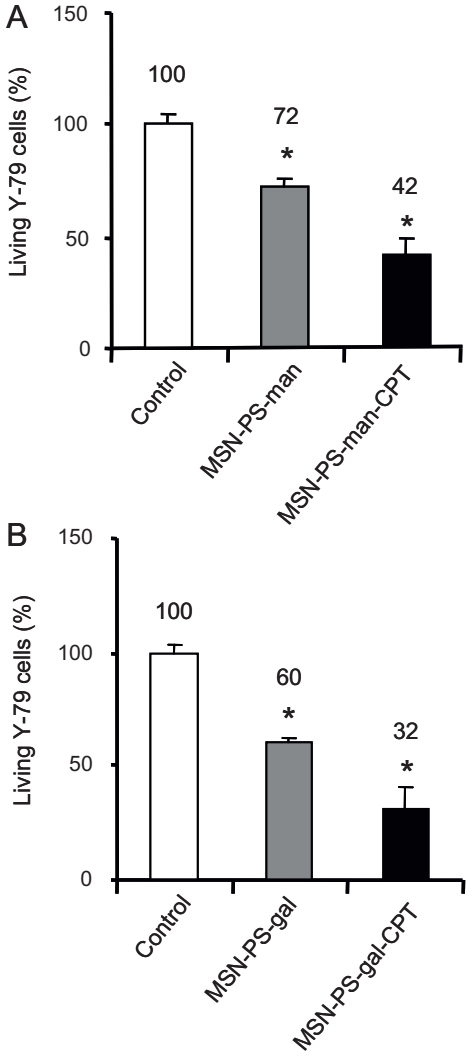

Fig. 2. Additional effect of PDT and drug delivery on retinoblastoma cells. Y-79 cells were incubated or not (control) with 20 μg mL^{-1} of (A) **MSN-PS-man** or **MSN-PS-man-CPT**; or (B) **MSN-PS-gal** or **MSN-PS-gal-CPT** for 24 h and then submitted to laser irradiation (λ = 650 nm, 90 J cm^{-2}). Cells were allowed to grow for 2 days and cell viability was quantified. Data are mean ± SD of 3 independent experiments. *$p < 0.05$ statistically different from control.

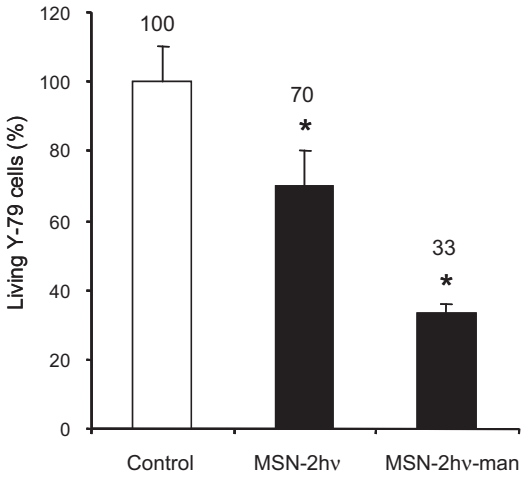

Fig. 3. TPE photodynamic efficiency on retinoblastoma cell line. Y-79 cells were incubated for 24 h with 20 μg mL^{-1} **MSN-2h*ν*** or **MSN-2h*ν*-man** and then irradiated at 760 nm, for 3× 1.25 s. Living cells are measured by MTS assay 2 days after irradiation. Values represent means ± SD of 3 experiments. Statistically different (Student's *t* test): *$p < 0.05$ from control.

20 μg mL^{-1} MSN-PS were not toxic in the dark and that irradiation alone was not toxic for cells (data not shown).

As shown in Fig. 2, monophotonic irradiation of Y-79 treated with **MSN-PS-man** induced 28% cell death. In contrast, when irradiated, **MSN-PS-man-CPT** induced 58% of cell death (Fig. 2A). The same experiment was realized with **MSN-PS-gal** and **MSN-PS-gal-CPT**. Results showed that **MSN-PS-gal** and **MSN-PS-gal-CPT** induced 40% and 68% of cell death, after irradiation respectively. These data demonstrate the high therapeutic potential of a synergistic use of drug delivery and PDT using the same MSN. This may represent an alternative strategy in the context of poorly responsive tumors to current therapies.

3.4. Mannose-functionalized MSN for TPE-PDT

TPE-PDT experiments using MSN functionalized or not with mannose were performed on the retinoblastoma Y-79 cell line. Cells were seeded in a 384-multiwell plate with 0.17 mm glass bottom and incubated with low concentrations of **MSN-2h*ν*** and **MSN-2h*ν*-man** (20 μg mL^{-1}) for 24 h. Two-photon irradiation was then performed on a confocal microscope equipped with a mode-locked Ti:sapphire laser at 760 nm by 3 scans of 1.25 s each at an average power of 80 mW (as described in Section 2) and the surface of the scanned areas was 1.5 mm × 1.5 mm (mean energy of 10.6 J cm^{-2}). Two days after irradiation, the percentage of living cells was determined by MTS enzymatic assay.

The nanoparticles were found to be non toxic without irradiation and irradiation alone did not damage the cells (data not shown).

As shown in Fig. 3, the photodynamic therapeutic potential of the MSN functionalized with mannose is clearly higher (67% of cell death) than that of unfunctionalized ones (30% of cell death) probably due to an active endocytosis of **MSN-2h*ν*-man** by Y-79 cells involving mannose receptors. This result is consistent with previous data indicating that mannosylated porphyrins were more efficient than non-functionalized ones for OPE-PDT *in vitro* and *in vivo* and the involvement of mannose receptors was postulated (Laville et al., 2006; Lupu et al., 2009).

In our study, TPE-PDT with **MSN-2h*ν*-man** led to a better efficiency compared to OPE-PDT with **MSN-PS-man**. This effect could be due to two different pathways of cancer cell death. Indeed the photosensitizers and excitation modes are different which could

lead to two different mechanisms of PDT. The production of reactive oxygen species and singlet oxygen with type I and type II mechanisms are known to be involved with OPE-PDT (Robertson et al., 2009). With TPE-PDT, Houde and co-workers (Mir et al., 2008) based on an interesting study of copper and zinc phthalocyanines have concluded that the triplet T_n excited state of a photosensitizer can be populated by TPE, which could lead to a type III process involving the production of reactive species.

4. Conclusion

Treatment studies on RB Y-79 cell line were carried out using multifunctionalized MSN anchored with carbohydrates. Confocal microscopy efficiently demonstrated the active endocytosis of the MSN which was mediated through carbohydrate receptors. TPE-PDT was performed using especially designed MSN for TPE and very promising results were observed with MSN functionalized with mannose, since a strong cell death was obtained after only a short irradiation at a low fluence. Alternatively, MSN allowing OPE-PDT combined with camptothecin delivery demonstrated a significant therapeutic synergy of these approaches to kill cancer cells. Thus, these data provide new evidences of the potential of functionalized and targeted MSN for the treatment of retinoblastoma and could lead to propose a non-invasive therapy with reduced side-effects.

Acknowledgements

Financial support by ANR PNANO 07-102, GDR "GDR CNRS 3049 Photomed "Médicaments photoactivables – Photochimiothérapie", Association pour la Recherche sur le Cancer" n° SFI20101201906 and the non profit organization Rétinostop is gratefully acknowledged. MM and CR fellowships were supported by Montpellier 2 University and Région Bretagne, respectively. We gratefully thank Michel Gleizes for technical assistance, Emmanuel Schaub from PIXEL platform (multiphotonic microscopy facilities, University of Rennes 1) and the Montpellier RIO imaging platform.

References

Aerts, I., Lumbroso-Le Rouic, L., Gauthier-Villars, M., Brisse, H., Doz, F., Desjardins, L., 2006. Retinoblastoma. Orphanet J. Rare Dis. 1.

Aerts, I., Pacquement, H., Doz, F., Mosseri, V., Desjardins, L., Sastre, X., Michon, J., Rodriguez, J., Schlienger, P., Zucker, J.M., Quintana, E., 2004. Outcome of second malignancies after retinoblastoma: a retrospective analysis of 25 patients treated at the Institut Curie. Eur. J. Cancer 40, 1522–1529.

Brevet, D., Gary-Bobo, M., Raehm, L., Richeter, S., Hocine, O., Amro, K., Loock, B., Couleaud, P., Frochot, C., Morere, A., Maillard, P., Garcia, M., Durand, J.O., 2009. Mannose-targeted mesoporous silica nanoparticles for photodynamic therapy. Chem. Commun., 1475–1477.

Chantada, G.L., Fandino, A.C., Raslawski, E.C., Manzitti, J., de Davila, M.T.G., Casak, S.J., Scopinaro, M.J., Schvartzman, E., 2005. Experience with chemoreduction and focal therapy for intraocular retinoblastoma in a developing country. Pediatr. Blood Cancer 44, 455–460.

Cheng, S.-H., Hsieh, C.-C., Chen, N.-T., Chu, C.-H., Huang, C.-M., Chou, P.-T., Tseng, F.-G., Yang, C.-S., Mou, C.-Y., Lo, L-W, 2011. Well-defined mesoporous nanostructure modulates three-dimensional interface energy transfer for two-photon activated photodynamic therapy. Nano Today 6, 552–563.

Collins, H.A., Khurana, M., Moriyama, E.H., Mariampillai, A., Dahlstedt, E., Balaz, M., Kuimova, M.K., Drobizhev, M., Yang, V.X.D., Phillips, D., Rebane, A., Wilson, B.C., Anderson, H.L., 2008. Blood-vessel closure using photosensitizers engineered for two-photon excitation. Nat. Photon. 2, 420–424.

Doz, F., 2006. Retinoblatoma: a review. Arch. Pédiatr. 13, 1329–1337.

Friend, S.H., Bernards, R., Rogelj, S., Weinberg, R.A., Rapaport, J.M., Albert, D.M., Dryja, T.P., 1986. A human DNA segment with properties of the gene that predisposes to retinoblastoma and osteosarcoma. Nature 323, 643–646.

Gary-Bobo, M., Hocine, O., Brevet, D., Maynadier, M., Raehm, L., Richeter, S., Charasson, V., Loock, B., Morere, A., Maillard, P., Garcia, M., Durand, J.-O., 2012. Cancer therapy improvement with mesoporous silica nanoparticles combining targeting, drug delivery and PDT. Int. J. Pharm. 423, 509–515.

Gary-Bobo, M., Mir, Y., Rouxel, C., Brevet, D., Basile, I., Maynadier, M., Vaillant, O., Mongin, O., Blanchard-Desce, M., Morere, A., Garcia, M., Durand, J.-O., Raehm, L., 2011. Mannose-functionalized mesoporous silica nanoparticles for efficient two-photon photodynamic therapy of solid tumors. Angew. Chem. Int. Ed. 50, 11425–11429.

Griegel, S., Rajewsky, M.F., Ciesiolka, T., Gabius, H.J., 1989. Endogenous sugar receptor (lectin) profiles of human retinoblastoma and retinoblast cell-lines analyzed by cytological markers, affinity-chromatography and neoglycoprotein-targeted photolysis. Anticancer Res. 9, 723–730.

Hocine, O., Gary-Bobo, M., Brevet, D., Maynadier, M., Fontanel, S., Raehm, L., Richeter, S., Loock, B., Couleaud, P., Frochot, C., Charnay, C., Derrien, G., Smaihi, M., Sahmoune, A., Morere, A., Maillard, P., Garcia, M., Durand, J.-O., 2010. Silicalites and mesoporous silica nanoparticles for photodynamic therapy. Int. J. Pharm. 402, 221–230.

Houston, S.K., Murray, T.G., Wolfe, S.Q., Fernandes, C.E., 2011. Current update on retinoblastoma. Int. Ophthalmol. Clin. 51, 77–91.

Khurana, M., Moriyama, E.H., Mariampillai, A., Samkoe, K., Cramb, D., Wilson, B.C., 2009. Drug and light dose responses to focal photodynamic therapy of single blood vessels in vivo. J. Biomed. Opt. 14.

Kleinerman, R.A., Tucker, M.A., Tarone, R.E., Abramson, D.H., Seddon, J.M., Stovall, M., Li, F.P., Fraumeni, J.F., 2005. Risk of new cancers after radiotherapy in long-term survivors of retinoblastoma: an extended follow-up. J. Clin. Oncol. 23, 2272–2279.

Laville, I., Pigaglio, S., Blais, J.C., Doz, F., Loock, B., Maillard, P., Grierson, D.S., Blais, J., 2006. Photodynamic efficiency of diethylene glycol-linked glycoconjugated porphyrins in human retinoblastoma cells. J. Med. Chem. 49, 2558–2567.

Levy, C., Doz, F., Quintana, E., Pacquement, H., Michon, J., Schlienger, P., Validire, P., Asselain, B., Desjardins, L., Zucker, J.M., 1998. Role of chemotherapy alone or in combination with hyperthermia in the primary treatment of intraocular retinoblastoma: preliminary results. Br. J. Ophthalmol. 82, 1154–1158.

Liong, M., Lu, J., Kovochich, M., Xia, T., Ruehm, S.G., Nel, A.E., Tamanoi, F., Zink, J.I., 2008. Multifunctional inorganic nanoparticles for imaging, targeting, and drug delivery. ACS Nano 2, 889–896.

Lu, J., Liong, M., Zink, J.I., Tamanoi, F., 2007. Mesoporous silica nanoparticles as a delivery system for hydrophobic anticancer drugs. Small 3, 1341–1346.

Lumbroso, L., Doz, F., Urbieta, M., Levy, C., Bours, D., Asselain, B., Vedrenne, J., Zucker, J.M., Desjardins, L., 2002. Chemothermotherapy in the management of retinoblastoma. Ophthalmology 109, 1130–1136.

Lupu, M., Thomas, C.D., Maillard, P., Loock, B., Chauvin, B., Aerts, I., Croisy, A., Belloir, E., Volk, A., Mispelter, J., 2009. ^{23}Na MRI longitudinal follow-up of PDT in a xenograft model of human retinoblastoma. Photodiag. Photodyn. Ther. 6, 214–220.

Mir, Y., van Lier, J.E., Paquette, B., Houde, D., 2008. Oxygen dependence of two-photon activation of zinc and copper phthalocyanine tetrasulfonate in Jurkat cells. Photochem. Photobiol. 84, 1182–1186.

Murphree, A.L., Villablanca, J.G., Deegan, W.F., Sato, J.K., Malogolowkin, M., Fisher, A., Parker, R., Reed, E., Gamer, C.J., 1996. Chemotherapy plus local treatment in the management of intraocular retinoblastoma. Arch. Ophthalmol. 114, 1348–1356.

Robertson, C.A., Evans, D.H., Abraharnse, H., 2009. Photodynamic therapy (PDT): a short review on cellular mechanisms and cancer research applications for PDT. J. Photochem. Photobiol. B: Biol. 96, 1–8.

Rodriguez-Galindo, C., Wilson, M.W., Haik, B.G., Merchant, T.E., Billups, C.A., Shah, N., Cain, A., Langston, J., Lipson, M., Kun, L.E., Pratt, C.B., 2003. Treatment of intraocular retinoblastoma with vincristine and carboplatin. J. Clin. Oncol. 21, 2019–2025.

Rosenholm, J.M., Sahlgren, C., Linden, M., 2010. Towards multifunctional, targeted drug delivery systems using mesoporous silica nanoparticles – opportunities & challenges. Nanoscale 2, 1870–1883.

Shields, C.L., Meadows, A.T., Shields, J.A., Carvalho, C., Smith, A.F., 2001a. Chemoreduction for retinoblastoma may prevent intracranial neuroblastic malignancy (trilateral retinoblastoma). Arch. Ophthalmol. 119, 1269–1272.

Shields, C.L., Shields, J.A., Cater, J., Othmane, I., Singh, A.D., Micaily, B., 2001b. Plaque radiotherapy for retinoblastoma – long-term tumor control and treatment complications in 208 tumors. Ophthalmology 108, 2116–2121.

Shields, J.A., Shields, C.L., Depotter, P., 1993. Cryotherapy for retinoblastoma. Int. Ophthalmol. Clin. 33, 101–105.

Slowing, I.I., Vivero-Escoto, J.L., Trewyn, B.G., Lin, V.S.Y., 2010. Mesoporous silica nanoparticles: structural design and applications. J. Mater. Chem. 20, 7924–7937.

Starkey, J.R., Rebane, A.K., Drobizhev, M.A., Meng, F.Q., Gong, A.J., Elliott, A., McInnerney, K., Spangler, C.W., 2008. New two-photon activated photodynamic therapy sensitizers induce xenograft tumor regressions after near-IR laser treatment through the body of the host mouse. Clin. Cancer Res. 14, 6564–6573.

Vezenkov, L.L., Maynadier, M., Hernandez, J.-F., Averlant-Petit, M.-C., Fabre, O., Benedetti, E., Garcia, M., Martinez, J., Amblard, M., 2010. Noncationic dipeptide mimic oligomers as cell penetrating nonpeptides (CPNP). Bioconjug. Chem. 21, 1850–1854.

Wong, F.L., Boice, J.D., Abramson, D.H., Tarone, R.E., Kleinerman, R.A., Stovall, M., Goldman, M.B., Seddon, J.M., Tarbell, N., Fraumeni, J.F., Li, F.P., 1997. Cancer incidence after retinoblastoma – radiation dose and sarcoma risk. J. Am. Med. Assoc. 278, 1262–1267.